PRACE INSTYTUTU ODLEWNICTWA

Tom XLIX **Rok 2009** **Zeszyt 1**

DOI: 10.7356/iod.2009.1

COMPARATIVE STUDIES OF THE EFFECT OF VARIOUS ADDITIVES ON STRUCTURE AND MECHANICAL PROPERTIES OF CuAl10Fe3Mn2 ALLOY

BADANIA PORÓWNAWCZE WPŁYWU RÓŻNYCH DODATKÓW NA STRUKTURĘ I WŁAŚCIWOŚCI MECHANICZNE STOPU CuAl10Fe3Mn2

Andrzej Gazda, Zbigniew Górny, Stanisława Kluska-Nawarecka, Henryk Połcik, Małgorzata Warmuzek

Instytut Odlewnictwa, ul. Zakopiańska 73, 30-418 Kraków

Abstract

Comparative studies were made on modification of aluminium CuAl10Fe3Mn2 bronze by application of modifiers affecting changes in surface properties (Na, K, Ca, Mg) and providing additional substrates for crystallisation (Zr, Ti, B). The results of structure examinations (optical microscope and scanning electron microscope), solidification kinetics analysis (thermal analysis), dilatometry, calorimetry, and mechanical tests were used.

Keywords: comperative studies, aluminium bronzes, modification, solidification, mechanical properties, structure

Streszczenie

Prowadzono badania porównawcze modyfikacji brązu aluminiowego CuAl10Fe3Mn2, stosując modyfikatory powodujące zmiany właściwości powierzchniowych (Na, K, Ca, Mg), jak również powstawanie dodatkowych miejsc krystalizacji (Zr, Ti, B). Wykorzystano wyniki badania struktury prowadzone techniką mikroskopii optycznej i skaningowej mikroskopii elektronowej, analizę kinetyki krzepnięcia (analiza termiczna), dylatometrię, kalorymetrię i wyniki badania właściwości mechanicznych.

Słowa kluczowe: badania porównawcze brązów aluminiowych, modyfikacja, krzepnięcie, właściwości mechaniczne, struktura

Introduction

Modification of copper alloys, the effects of grain refining included, goes back to the fifties of past century [1, 2]. First attempts were related with grain refining of tin and tin-zinc bronzes, using additives of Zr, Ti, Fe, Co, B, Cr and Mn or P [3–6].
Refining of grains in common and special-purpose brasses (of aluminium and silicon type) has been investigated and partially used in foundry industry; the refining is done with additives of Zr, B, Fe, C, Mg, P or Ti [1, 7–12]. The effect of Fe, Li, Bi and Sb on copper structure [9] and of Zr in silicon bronzes was also examined [13]. All these investigations and treatments concerned one of the possible techniques of alloy modification, which consists in the formation of additional crystallisation substrates, frequently resulting in structure changing from the columnar into equiaxial with the accompanying effect of grain refinement [14].

Some investigations were also carried out on the modification of CuSn10 alloy with additives of Ca, obtaining slight improvement of mechanical properties (R_m) and high level of plastic properties (A, Z) with some spheroidisation of grains in the solid solution α in a Cu-Sn system [15].

As regards aluminium bronzes, the information on their modification is very scarce. Those were mainly some attempts at introducing the nuclei-forming addtives, like V, Ti, B or Zr to CuAl9Fe3 alloy [16] and of Ca [17], which is changing the surface properties through change of the surface tension and wetting angle. Some investigations were also undertaken in respect of CuAl10Fe3Mn2 alloy and silicon bronze (with additions of Zn and Mn), with the resultant increase of mechanical and plastic properties and improved resistance to cavitation erosion and corrosion in seawater. The addition of Ca is, moreover, considered to act as a deoxidiser and desulphuriser [18].

1.The research concept and background

A comparative study was done for two types of modifiers, viz. the modifiers that are changing surface properties and those which produce additional substrates of crystallisation. In the choice of the modifiers of the first type, based on the theory of electrons, a characteristic feature of the material ability - to release free electrons - can be its thermionic work function, electronegativity, the ionising potential, or the effective ionising potential [19]. All substances with the value of electronegativity or of the effective ionising potential U lower than that of the metallic alloy matrix possess some modifying power:

$$U_{Me} - U_{Mod} > 0 \quad (1)$$

The second factor characteristic of the modifying power of an additive is its limited solid state solubility:

$$C_s < 0.1 \text{ at. \%} \quad (2)$$

Both these typical features can be combined in one expression called "coefficient of the modifying effect".

$$\mu = (U_{Me} - U_{Mod})/C_s \quad (3)$$

for modifiers μ>1. In practice, the following ranges are adopted:

no significant effect on crystallisation	μ = 0–10
modest effect	μ = 10–100
strong modifying effect	μ = 100

The next factor which decides about the choice of a modifier of this type is the surface tension δ, and strictly speaking, the difference in surface tensions of the modifier and copper (when modifying copper alloys), that is:

$$\Delta\sigma = \sigma_{Mod} - \sigma_{Cu} \tag{4}$$

Equation (4) should have a negative value. The difference between the first derivatives of surface tension can be examined as well:

$$\Delta\frac{d\sigma}{dt} = \left(\frac{d\sigma}{dt}\right)_{Mod} - \left(dt\frac{d\sigma}{dt}\right)_{Cu} \tag{5}$$

From the property data of the elements, compiled in a respective table, it follows that the suitable values of μ possess the following elements: K (25 333), Na (590), Cs (88 000), Sr (1567), Ba (580), La (245); calcium examined previously has the value of 74, and so it is placed in the group of μ = 10–100, that is, in the group of modifiers with very modest effect. Being widely available, Na, K and Ca have been chosen for the examinations, the latter one having already been the subject of investigations described in [18]. From among the modifiers which are said to produce the additional substrates of crystallisation in liquid metal, it has been decided to choose Zr, Ti and B as additives used for various Cu alloys. Thus, the comparative studies have covered alloys with the following alternative additives:

A - without modifiers
B - 0.004% Na
C - 0.001% K
D - 0.060% Zr
E - 0.034% Ti
F - 0.086% Ca and 0.048% Mg
G - 0.11% Ca
H - 0.010% B

The investigations were carried out at two stages. At stage I, using a ball-shaped specimen (Fig. 1) and the results of solidification kinetics analysis (thermal analysis), structure examinations (optical microscope and SEM), dilatometry and calorimetry, the effect of various additives on the structure was evaluated.

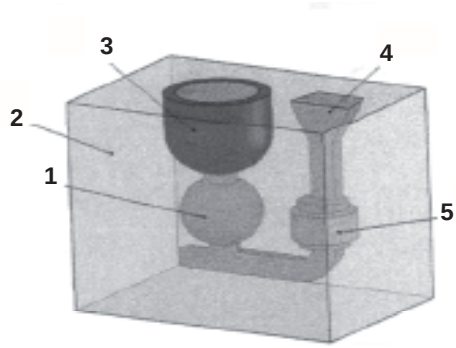

Fig. 1. Model of test casting for structure examination of CuAl10Fe3Mn2 alloy: 1 - casting, 2 - die, 3 - insulation, 4 - gating system, 5 - filter

Rys. 1. Model odlewu próbnego do badania struktury stopu CuAl10Fe3Mn2: 1 - odlew, 2 - kokila, 3 - izolacja, 4 - układ wlewowy, 5 - filtr

At stage II, using some selected additives, i.e. Na,K and Ca, the mechanical properties (R_m, $R_{0,2}$, A, Z, HB) were tested on the specimens cast separately (Fig. 2).

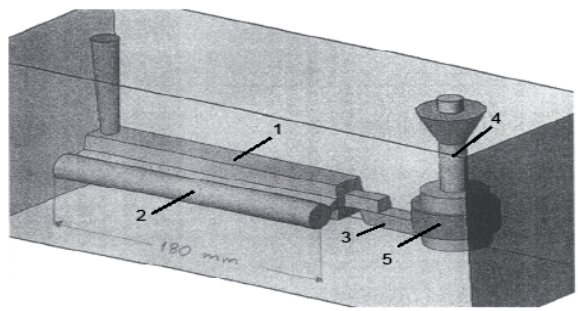

Fig. 2. Model of cast specimen for mechanical testing of CuAl10Fe3Mn2 alloy: 1 - cross runner, 2 - specimen, 3 - strain relief, 4 - gate, 5 - filter

Rys. 2. Model odlanej próbki do badania właściwości mechanicznych stopu CuAl10Fe3Mn2: 1 - belka wlewowa, 2 - próbka, 3 - przelew, 4 - wlew, 5 - filtr

2. Test conditions

The charge was composed of pigs delivered by Hutmen Wrocław, characterised by the following composition: CuAl10.06Fe3.06Mn1.56 (Sn 0.06, Zr 0.20, Pb 0.03, Ni 0.03, Si 0.04, P 0.05, Sb 0.01, Bi 0.005, As 0.006, Mg 0.005, S up to 0.1, and O_2 up to 0.0024%).

The test balls (1) were gravity cast into dies, into sand moulds made from sodium silicate sand with resin hardener (MM-1001E resin), and into sand moulds with high (75%) content of an insulating material (granulated kaolinite), used as a facing sand (a layer of 3–4 cm thickness). The points of temperature measurement (thermocouples) are schematically shown in Figure 3.

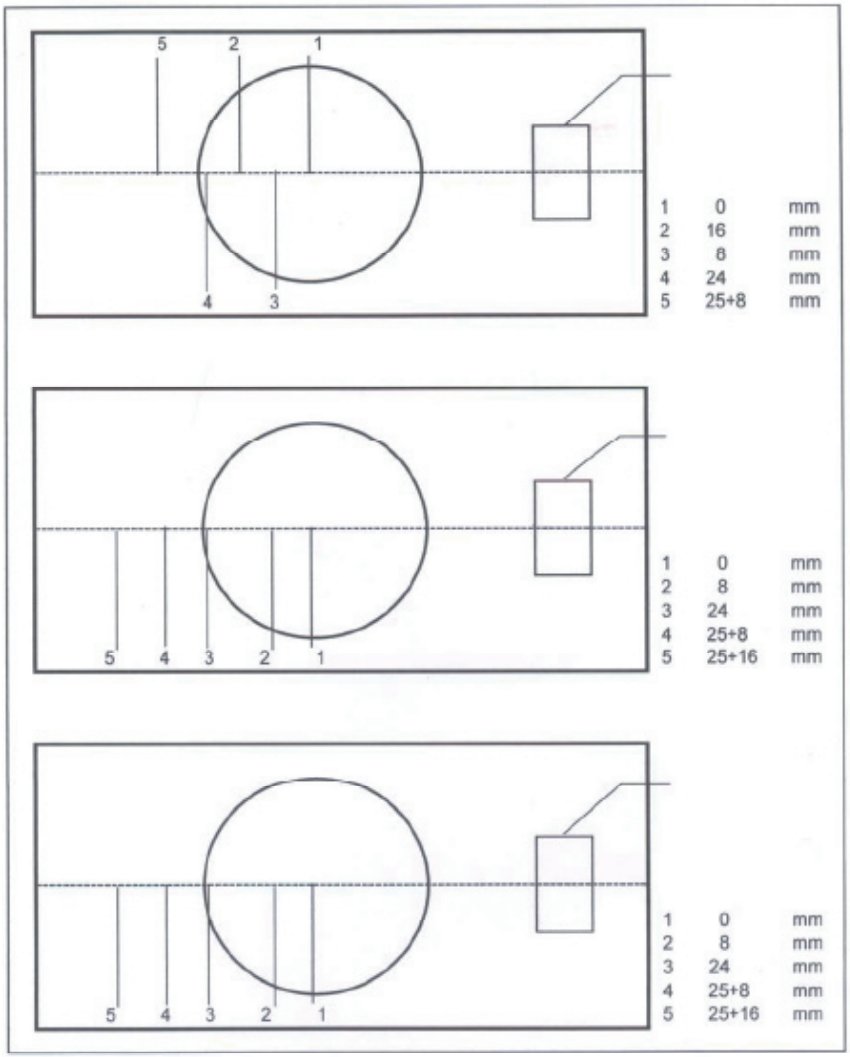

Fig. 3. Location of thermocouples: A - die, B - sand mould, C - mould with insulating layer, D - gating system, E - thermocuple position In respekt of the ball centre (test casting)

Rys. 3. Umiejscowienie termopar: A - kokila, B - forma piaskowa, C - forma z warstwą izolującą, D - układ wlewowy, E - lokalizacja termopary w odniesieniu do środka kuli (odlew próbny)

The modifying additives were delivered by Sigma-Aldrich (Poznań) and comprised the following materials:

- potassium rods of Φ 25,
- calcium granules 6,
- sodium bars.

Moreover, the master alloys of CuZr30, CuTi30 and CuB2 used in the experiments were delivered by KBM Affilips Master Alloy.

Temperature measurements (in mould and casting) were taken with NiCr-Ni thermocouples (type K) of 0.4 mm diameter, recalibrated by reference to a Pt-PtRh10 thermocouple checked at the Regional Verification Office in Warsaw. A 15-channel MrAC-15 recorder made by Jota with in-built linearisation system was used.

The charge was melted in a high-frequency induction furnace (Radyne AMF/45) of 2.3 kHz frequency with a crucible of 50 kg capacity. Double deoxidising treatment was applied, viz. with phosphor copper after overheating of molten alloy (CuP10 or CuP15), and with an addition of magnesium after refining with compressed nitrogen.

Microstructure was examined under a Neophot 32 optical metallographic microscope at magnifications of 50x, 100x and 500x; the specimens were etched with a reagent of the following composition: 10 ml Na_4OH, 20 ml H_2O i 4 ml H_2O_2 (3%).
The evaluation of microstructure was done:

- by a comparative method in accordance with PN-H-87902:1972, determining the degree of eutectic structure refinement and volume content of phase β (β'),
- by the secant method (Heyn's method) in accordance with PN-EN ISO 2624:1997.

The dilatometry, done in order to examine the solid state transformations, was carried out on a Linseis L75 dilatometer (specimens of Φ 30x30 mm, argon, 20–900°C, heating rate of 10 K/mm).

The random calorimetric examinations were done by the method of differential scanning calorimetry DSC, using a Netzch 404 Pegasus calorimeter (20–900°C, argon vacuum, 10 K/mm).

3. Discussion of results

3.1. Chemical analysis

The chemical analysis was done at the Stanisław Staszic Institute for Ferrous Metallurgy in Gliwice. Basing on the results of the charge and cast samples analysis, the following melting loss of the additives was calculated: Al - 2.7%, Mn - 3.2%, Na - 96%, K - 99.2%, Ca+Mg - 96.6%, Ca - 26.7%, Zr 0.0%, Ti - 32%, and B - 50%.

3.2. The cooling curves

The cooling curves differed considerably for castings made in dies and in sand moulds, this also referring to castings made in moulds with insulating material – Figure 4.

The runs of the curves plotted for a sample of metal and for mould are typical, although they illustrate different kinetics of solidification (the rate of solidification and cooling). A characteristic feature is the length of eutectic arrest (Tab. 1) obtained for the centre of test casting (point 1 on the cooling curves). There are some obvious differences in arrest times, depending on the heat transfer rate in die (16–20 s), in sand mould (60–80 s), and in mould with insulating layer (70–150 s), the differences being relatively smaller for die castings.

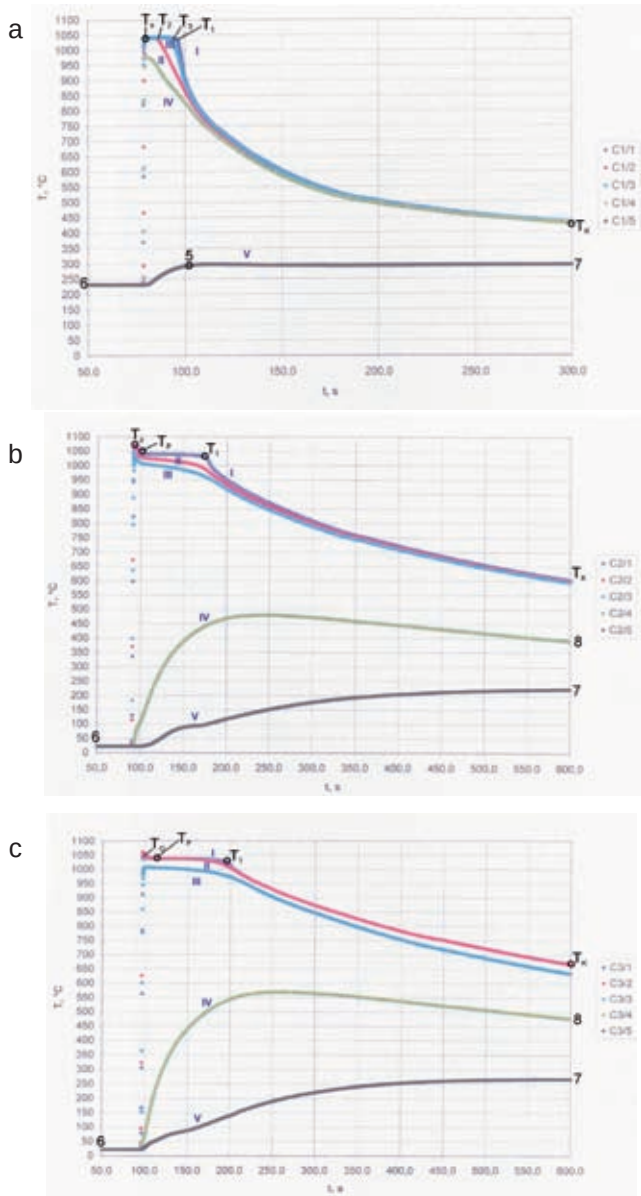

Fig. 4. Cooling curves of testing casting (melt C): a - gravity die cast, b - sand cast, c - cast in mould with insulating layer; 1, 2, 3 - measuring points as in Fig. 3, o - beginning of eutectict arrest, p - beginning of recording, 6, 7 - beginning and end of mould temperature curve (curve for points 5 - Fig. 3), 8 - mould temperature curve run at point 4 (Fig. 3)

Rys. 4. Krzywe stygnięcia dla odlewu próbnego (wytop C): a - odlewanie kokilowe, b - odlewanie w masie piaskowej, c - odlewanie w formie z warstwą izolującą; 1, 2, 3 - punkty pomiarowe jak na rys. 3, o - początek przystanku eutektycznego, p - początek rejestrowania danych, 6, 7 - początek i koniec krzywej temperatury formy (krzywa dla punktu 5 - rys. 3), 8 - krzywa temperatury formy poprowadzona w punkcie 4 (rys. 3)

Table 1. Time of solidification (t_1-t_p) and length of eutectic arrest (t_1-t_o) according to Figure 4 for the centre of test casting (ball acc. to item 1) made from CuAl10Fe3Mn2 aluminium bronze with different modifying additives

Tabela 1. Czas krzepnięcia (t_1-t_p) i długość przystanku eutektycznego (t_1-t_o) wg rysunku 4 dla środka odlewu próbnego (kula wg poz. 1) wykonanego z brązu aluminiowego CuAl10Fe3Mn2 z dodatkiem różnych modyfikatorów

Melt[1)]	Time till end of solidification: t_1-t_p, s			Length of eutectic arrest: t_1-t_o, s		
	Die	Sand mould	Insulated mould	Die	Sand mould	Insulated mould
A	34	100	100	19	74	75
B	211	295	350	17	85	110
C	97	180	190	18	80	90
D	87	170	200	17	80	100
E	38	100	150	12	60	100
F	86	180	300	20	100	150
G	48	150	220	18	105	130
H	123	210	310	19	70	150

[1)] A - non-modified melt, B - melt modified with sodium, C - with potassium, D - with zirconium, E - with titnium, F - with calcium and magnesium, G - with calcium, H - with boron

The run of the curves for the first derivatives (dT/dt) is shown in Figure 5. The arrests are distinctly visible, in a like manner as the solid state transformations (e.g. a eutectoid transformation $\beta \rightarrow \beta + \gamma_2$) for castings made in sand moulds and in moulds with insulating layer.

a

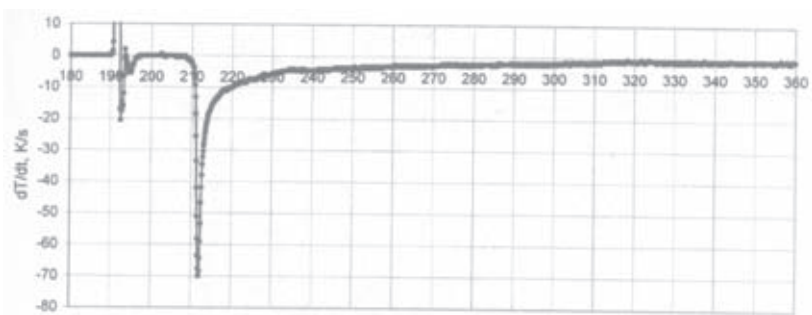

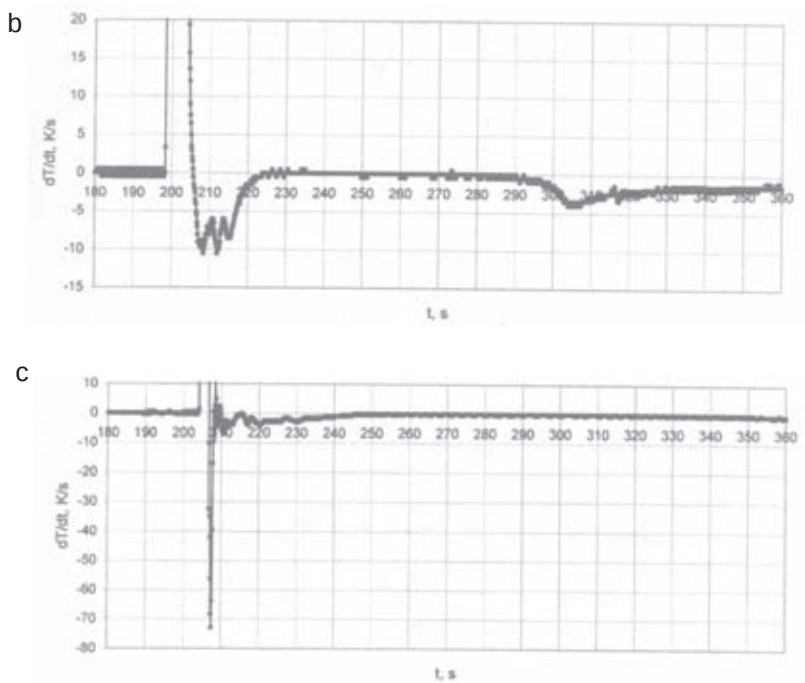

Fig. 5. Differental cooling and solidification curves (dT/dt) of melt B: a - die, b - sand mould, c - mould with insulating layer

Rys. 5. Krzywe różnicowe stygnięcia i krzepnięcia dT/dt) dla wytopu B: a - kokila, b - forma piaskowa, c - forma z warstwą izolującą

The gradient curves (Fig. 6) reveal the values of dT/dx decreasing gradually with the lapse of time, the differences between various runs of the curves are decreasing, too.

The run of the curves differs quite notably for dies and sand moulds. The difference is particularly visible in the case of gradient curve 1 > 2, characterised by quite different kinetics of the heat flux transfer.

a

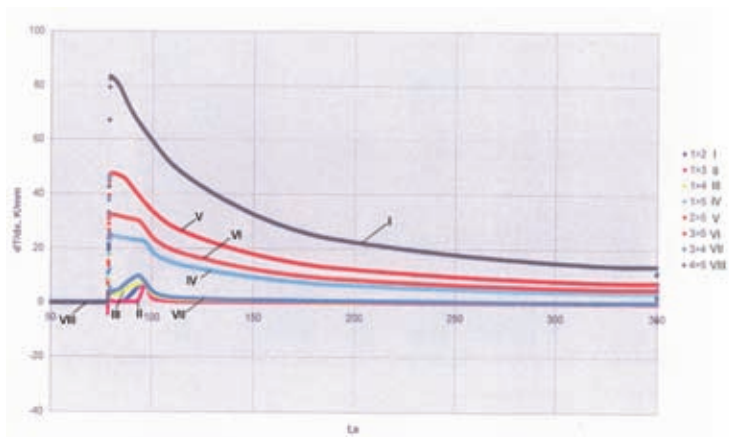

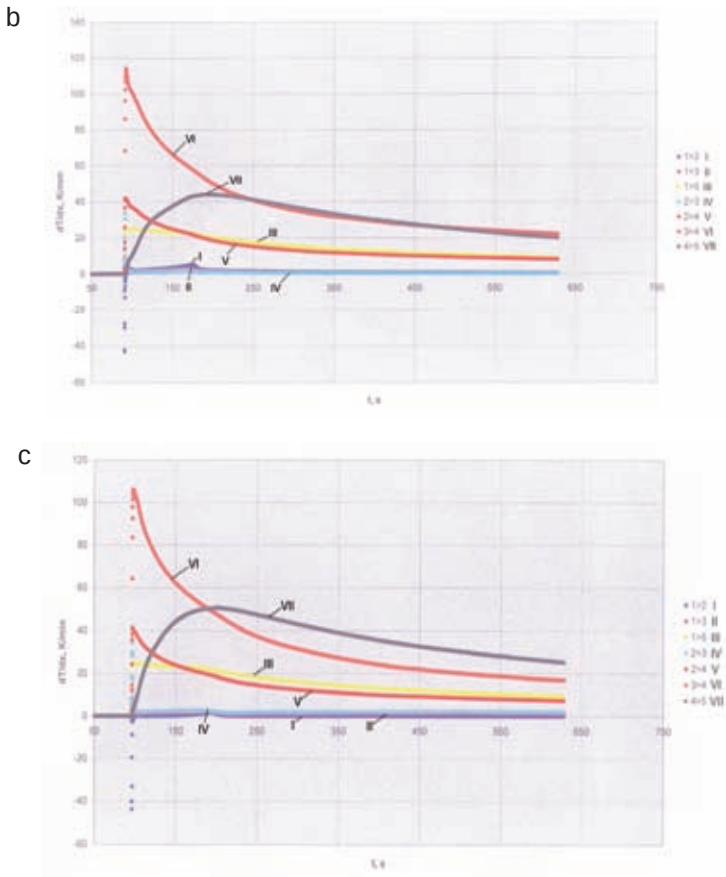

Fig. 6. Gradient curves of melt C: a - die, b - sand mould, c - mould with insulating layer

Rys. 6. Krzywe gradientowe dla wytopu C: a - kokila, b - forma piaskowa, c - forma z warstwą izolującą

3.3. Microstructure examinations

In the table 2 results of the estimation of the stereological parameters describing microstructure of the examined specimens: V_v (volume fraction of phase constituents) and S_v (specific area of the phase boundaries) have been presented.

The volume fraction of the high temperature β phase was slightly influenced by cooling rate, though its significant increase has been stated in specimens poured into metal mould. Only one except form this trend was observed in melt B in which there are not any visible difference among the examined specimens.

The microstructure in specimens cut from the cast parts poured into metal mould was more dispersed than that observed in sand cast parts and sand cast parts with insulating coating as well. However one can see that in melts F and H some decrease in the S_v value (i.e. less dispersed microstructure) has been occurred.

There are three series of the specimens cut from examined cast parts, formed according their decreasing microstructure dispersion:

- gravity die mould: B, C, H, A, D, G, E, F;
- sand mould casting: A, B, C, D, E,G, F, H;
- sand mould with insulating coating: A,B,C,D,E,G,H,F.

Table 2. Results of the measurements volume fraction of β phase V_v and specific area of the phase boundaries S_v (specimens designation: A - melt without modifying additives, B to H - melts modified with Na, K, Zr, Ti, Ca+Mg, Ca+B respectively, 1, 2, 3 - gravity die cast part, sand cast part, cast part in sand mould with special insulating coating, respectively)

Tablica 2. Wyniki pomiarów udziału objętościowego V_v fazy β oraz powierzchni właściwej granicy faz S_v (oznaczenie próbki: A - ciekły metal bez dodatków modyfikujących, B do H - ciekły metal modyfikowany, odpowiednio, Na, K, Zr, Ti, Ca+Mg, Ca+B , 1, 2, 3 - odpowiednio, odlew kokilowy, odlew wykonany w formie piaskowej i odlew wykonany w formie piaskowej ze specjalnym pokryciem izolującym

Melt	Sample	S_v [1] mm²/mm³	Volume fraction of β (β'), V_v
A	A1	139.2	F50
	A2	106.8	F10
	A3	104	F10
B	B1	178.4	F10
	B2	100	F10
	B3	93.2	F10
C	C1	164.8	F50
	C2	95.2	F10/50
	C3	88.8	F50
D	D1	135.6	F50
	D2	86	F50
	D3	75.2	F50
E	E1	130	F50/10
	E2	74	F10
	E3	64.4	F10
F	F1	118.8	F50
	F2	72	F10
	F3	57.6	F10
G	G1	135.6	F50
	G2	63.2	F10
	G3	59.6	F10
H	H1	140.8	F50
	H2	71.2	F10
	H3	59.6	F10

[1] S_v was estimated with linear method, in 5 fields of view, true length of the measure line: 250 μm

The differences between the effectiveness of modifiers type I (B, C, F, G) and type II (D, E, F), evaluated from the results of an analysis of the refinement degree dispersion, are small within the same casting process; there are, obviously, some differences between castings made in dies and sand moulds, or castings made in sand moulds with insulating layer.

Comparison at the revealed differences in dispersion degree observed in the examined specimeses enabled revealing the most important differences in the degree of macrostructure dispersion, specially for gravity die castings, among which melts B and C, i.e. the melts modified with sodium or potassium, are the most characteristic. It is also worth noting that melt A (non-modified and deoxidised only with phosphorus in the form of phosphor copper) reveals relatively high values of S_v, viz.139.2 - for dies, 106.8 - for sand moulds, and 104 for moulds with insulating material. The non-modified melt was cast at a temperature slightly higher than the modified melts with overheating to a relatively similar temperature (1220–1250°C) due to the modifying treatment.

During microstructural examinations, a more uniform distribution of the high-refined phases rich in Fe was observed in the case of melts modified with Na and K (Fig. 7), compared to other melts (e.g. melt D with an addition of Zr).

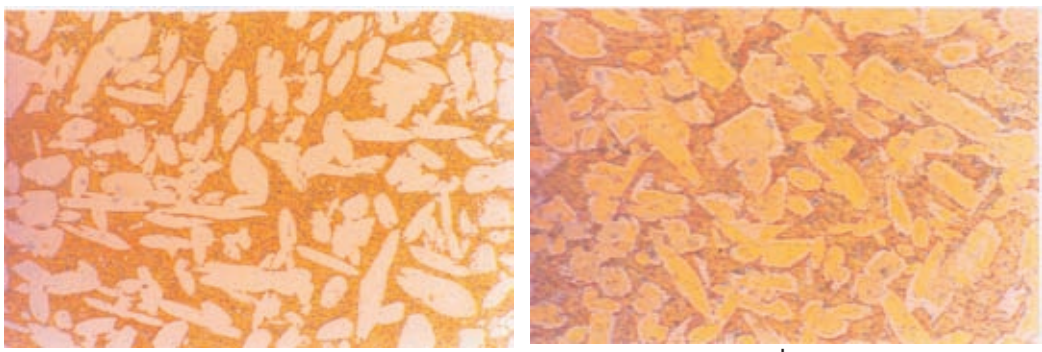

a b

Fig. 7. Microstructures of sand cast specimens (balls) from melts B (a) and D (b)

Rys. 7. Mikrostruktury próbek w kształcie kuli odlewanych w formach z masy piaskowej - metal z wytopów B (a) i D (b)

In the examinations carried out to identify the phases rich in Fe, the results of SEM and X-ray EDS microanalysis were used (Fig. 8 and Table 3). The phases rich in Fe have different forms of the precipitates (spherical, fine propellers, plates, barrels, trefoils, fine dendrites, and angular configurations), etching in blue, and large spherical precipitates which inside have other precipitates coloured in blue or dark brown; some needle-like precipitates are also present; they are so fine that only the grain boundaries are visible.

Phases rich in iron, designated as K in CuAlFeMn or CuAlFeNiMn alloys, can assume five different intermetallic forms, based on NiAl (K_3) Fe_3Al (K_2), Fe_3Al or NiAl (K_5) of B2 lattice (CsCl); sometimes they are described by a general formula of (Fe,Ni)Al and are designated as K [20–23]. Comparing the results in Table 3 with the data given in literature, a strong non-homogeneity of the precipitates of phase K is observed with certain analogy

to nickel-free phases of the K1 type (containing high volumes of Fe) or K3 type (with high content of Cu and a moderate content of Fe); the content of Mn in all the examined inclusions is relatively low and these phases rather contain a large volume of copper (stars, needles, rhombi, or spheroids, possibly also the narrow needles).

The situation is similar as regards phases K containing less iron than copper (K3) and present in the form of little stars or spheroids. Melts C,G and H were examined on samples cast in moulds with insulating layer, that is, on samples which have the lowest cooling rate, approaching the state of equilibrium with all the resultant consequences (the presence of eutectoid $\alpha + \gamma_2$).

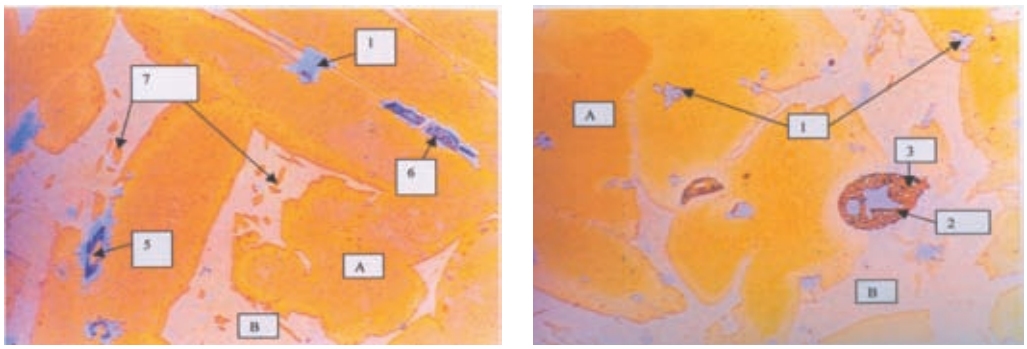

designations	A	B	1	2	3	4	5	6	7
microconstituent	ralpha phase	region of beta phase	star	precipitate in eutectoid	eutectoid	thin needle	rhombus	needle	needle in eutectoid

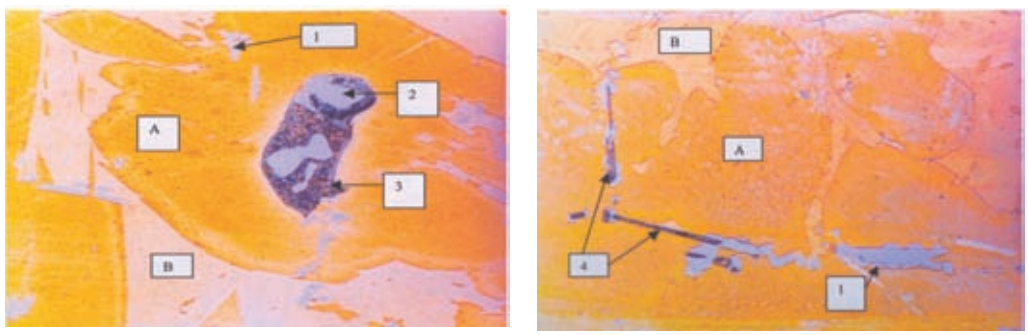

Fig. 8. Iron-rich phases as visible under SEM with EDS microanalysis

Rys. 8. Fazy bogate w żelazo - wyniki badania metodą skaningowej mikroskopii elektronowej (SEM) w połączeniu z mikroanalizą rentgenowską EDS

Table 3. The results of analysis of the chemical composition in microregions (the method of X-ray EDS microanalysis)

Tabela 3. Wyniki analizy składu chemicznego w mikroobszarach (metoda mikroanalizy rentgenowskiej EDS)

	Morphology of precipitates (place)	Measurement No.	Chemical composition, wt.%				
			Al	Mn	Fe	Cu	Other
C3 [1)]	Matrix (phase α) (A) [2)]	1	6.73	1.33	0.79	91.15	
		2	5.67	1.26	1.94	91.13	
	Phase β (B)	1	7.65	1.99	1.34	89.01	
		2	8.8.	1.95	1.03	88.22	
	Star (1)	1	7.23	2.88	65.96	21.70	Si
		2	6.81	3.01	71.16	16.97	Si
		3	7.60	2.17	23.37	61.99	Si
		4	7.66	2.36	30.57	58.70	Si
G3	Matrix (A)	1	5.40	1.28	1.72	91.61	
		2	5.86	1.24	1.59	91.30	
	Phase β (B)	1	8.64	2.06	0.83	88.47	
		2	8.25	1.91	0.71	89.12	
	Star (1)	1	7.48	3.16	60.73	26.66	Si
		2	8.53	2.27	20.20	68.99	
	Eutectoid α+γ_2 (3) α+K	1	4.48	1.81	13.01	63.89	Ca,Cr
		2	6.79	2.43	41.05	42.81	Si,Ca
H3	Matrix (A)	1	6.23	1.67	1.25	90.84	
		2	6.27	1.25	1.71	90.78	
	Phase β (B)	1	8.87	1.39	0.82	88.92	
		2	8.83	1.73	1.05	88.39	
	Star (1)	1	8.20	3.20	47.62	39.89	Si
		2	7.16	3.17	60.84	25.99	Si,P
		3	5.68	3.06	75.58	9.90	Si,Cr
		4	6.37	2.74	52.74	36.30	Si
	Needle (6)	1	1.77	4.06	81.65	9.83	Si,P
		2	2.29	3.27	80.03	12.42	Si
		3	2.29	2.84	89.82	5.24	
	Narrow needle (4)	1	4.63	2.57	35.30	55.54	Si,Cr
	Ball (2)	1	1.48	4.83	43.41	41.70	Si,Cr
	Rhombus (5)	1	1.98	3.77	71.81	18.46	Si,Cr

[1)] C,G,H: melts with an addition of sodium, calcium and boron, respectively, made in sand moulds with insulating layer

[2)] determined on microstructures

The kinetics of the test castings solidification and cooling to a pre-established temperature can be estimated from the mean values of solidification and cooling v_{sr} or from the mean values of cooling alone v'_{sr}, where:

$$v_{sr} = \frac{T_p - T_K}{t_K - t_p}; \frac{^oC}{s}; v'_r = \frac{T_l - T_K}{t_K};$$

The mean rate of mould heating can be estimated from:;

$$f_{śr} = \frac{T_7 \quad T_6}{t_K};\ ^\circ C/s$$

Figure 9 shows these mean rates as obtained for the individual melts. There are but only slight differences between the individual melts (v_{sv} and v'_{sv}), some insignificant differences between the values of v_{sr} and v'_{sr}, and slightly greater differences in the case of f_{sr}.

3.4. Dilatometric and calorimetric examinations

Since the test castings (balls) were knocked out from moulds at a temperature of about 600°C, some additional examinations were necessary to estimate the transformations in solid state, and specially the formation of eutectoid $\alpha + \gamma_2$ and/or pseudoeutectoid α + K. The dilatometric examinations enabled determination of the values of some typical phase transformation temperature along with the coefficient of thermal expansion $\beta(T\text{-}T_o) = \frac{\Delta L}{L(T \quad T_o)}$.

The results of the examinations were plotted in the form of curves illustrating functions $\Delta L/L = f(T)$ and $\beta (T\text{-}T_o) = f(T)$ (Fig. 10).

For all the examined samples, the relationship $\Delta L/L = f(T)$ assumes the shape of an approximately straight line (Fig. 10a). The run of function $\beta(T\text{-}T_o) = f(T)$ within the range of temperatures 200–400°C is reflecting the processes of precipitation and solid state dissolution of phases characterised by non-equilibrium composition, while an insignificant effect of growth at a temperature above 550°C may signal the occurrence of a eutectoid transformation type $\beta \rightarrow \alpha + \gamma_2$, possibly $\beta \rightarrow \alpha$ + K (Fig. 10b). At a temperature of about 380°C some changes are observed which result most probably from changes in the solubility; in melt D the low-temperature changes are insignificant. The change of volume accompanying these transformations is very small which proves that the content of these phases is low. The curve plotted in Fig.10 shows the derivatives $\delta(\Delta L/L)/\delta$ T in function of temperature. An arrow on the curves denotes the characteristic point of eutectoid transformation, while the hatched areas denote changes of volume. These are the temperatures above 550°C. With cooling proceeding more slowly, this point will shift to higher temperatures.

The calorimetric examinations were performed at random for melt B2. The DSC curve (Fig. 11) confirms the results of dilatometric examinations. On the DSC curve of preheating one can note (within the range of up to about 450°C) changes in the base (background) line, typical of the superposing processes of precipitation (from supersaturated solution) and phase dissolution, proceeding with preheating of the specimen (Fig. 11). The double endothermic effect is well visible (500.3 and 551.0°C), and it reflects the eutectoid transformation proceeding at a temperature of about 565°C (according to the phase equilibrium diagram).

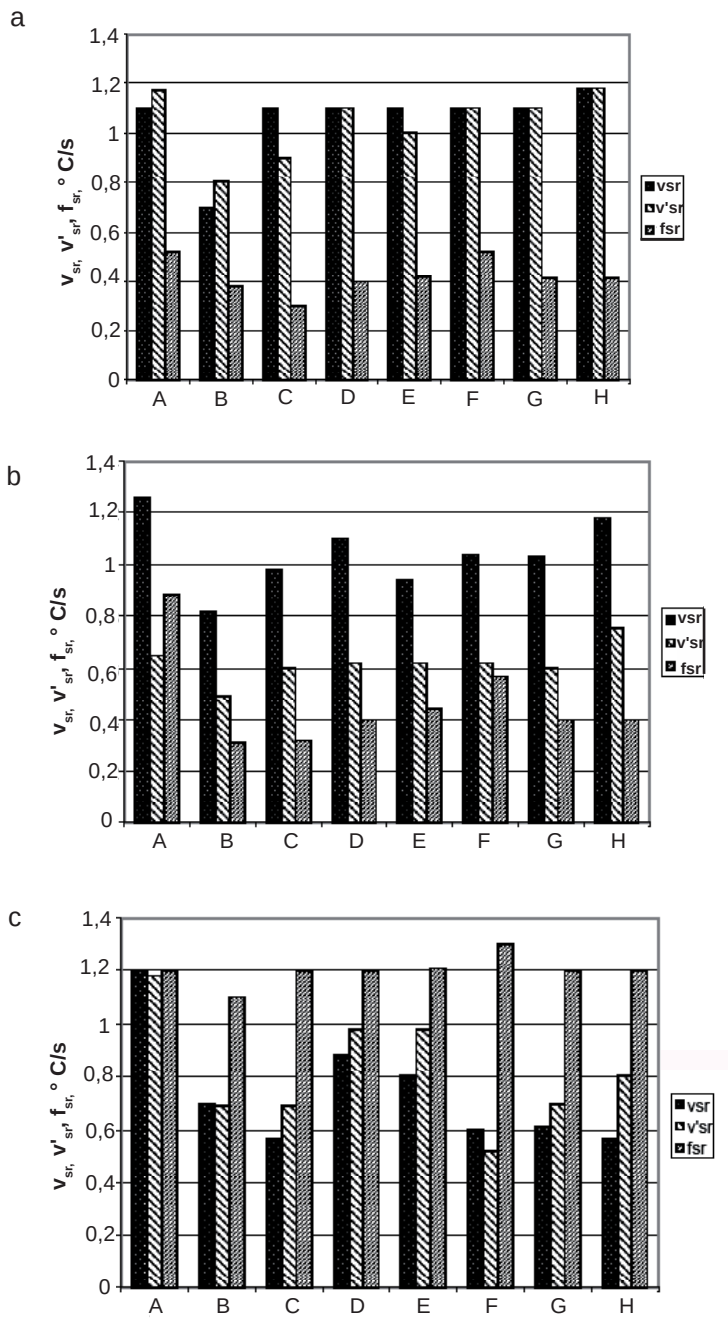

Fig. 9. Average rates of cooling (v'_{sr}), solidification and cooling (v_{sr}) and mould heating (f_{sr}) for gravity die casting (a), sand casting (b) and casting made in mould with insulating layer (c)

Rys. 9. Średnie szybkości stygnięcia (v'_{sr}), krzepnięcia i stygnięcia (v_{sr}) oraz ogrzewania formy (f_{sr}) dla procesu odlewania kokilowego (a), odlewania w formach piaskowych (b) i odlewania w formach w warstwą izolującą (c)

Analogical effects can be observed during cooling of B2 specimen in calorimeter; both effects, i.e. the solubility limit of phase α exceeded and the exothermic effect of eutectoid transformation starting at a temperature of about 520°C are well visible.

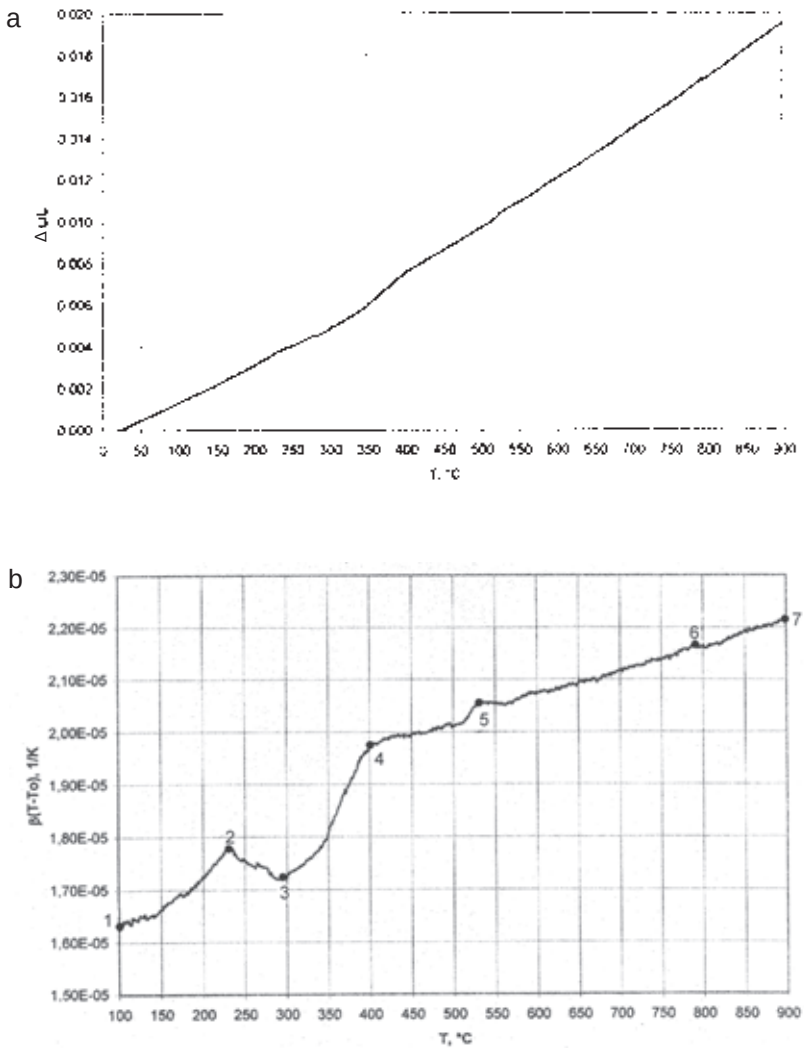

Fig. 10. Results of dilatometric measurements taken from melt B; sand cast specimens; a – ΔL/L = f(T); b - relationship between the first derivatives β and temperature melts C and D

Rys. 10. Wyniki pomiarów dylatometrycznych dla wytopu B; próbki odlewane w masie piaskowej; a – ΔL / L = f(T); b - współzależność pomiędzy pierwszą pochodną β i temperaturą dla wytopów C i D

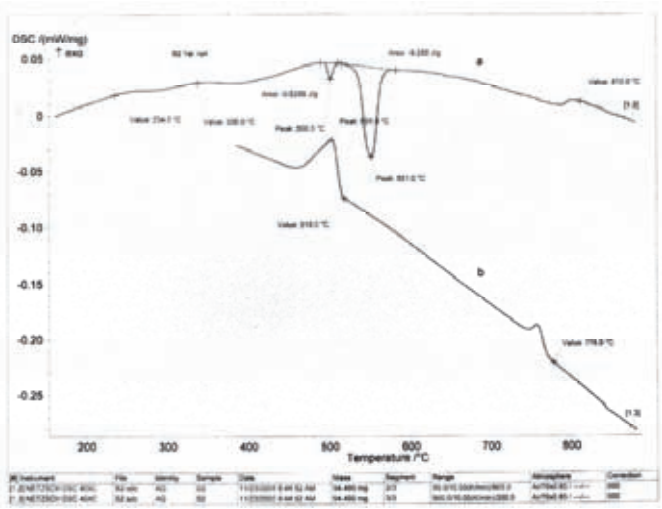

Fig. 11. Results of calometric measurements DSC = f(T) taken for melt B and sand cast specimen; a - heating, b - cooling

Rys. 11. Wyniki pomiarów kalorymetrycznych DSC = f(T) dla wytopu B i próbek odlewanych w masie piaskowej; a - ogrzewanie, b - stygnięcie

Figure 12 shows the phase equilibrium diagram with plotted equivalent composition of the examined alloy; for the determination of equivalent Al content. the following values have been adopted: 6 for Mn (1% Mn = 0.16% Al) and 1% Fe = 0.15% Al for Fe [24, 25]. Hence the equivalent content for CuAl10.06Fe3.06Mn1.56 is 10.06 + 0.46+ 0.23 = 10.75 (Fig. 12).

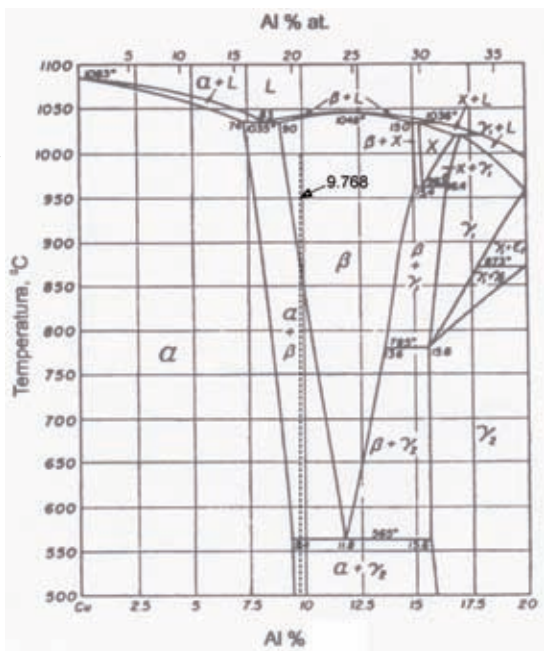

Fig. 12. Phase equilibrium diagram for Cu-Al system [26]; vertical straight line denotes equivalent aluminium content in the examined alloy

Rys. 12. Wykres równowagi fazowej dla układu Cu-Al [26]; pionowa linia prosta oznacza równoważną zawartość glinu w badanym stopie

3.5. Basic mechanical properties

Tests were performed on separately cast specimens (Fig. 2); the obtained results are compiled in Table 4. In the conducted series of tests (stage II), the effect of Na, K and Ca additives was investigated. The first two modifiers have proved to be relatively more efficient than the others, mainly due to a higher degree of dispersion (Table 2) as well as their beneficial effect on the uniform distribution of phases in structure and yielding precipitates of relatively smaller dimensions. The addition of Ca was introduced to compare the effect of Ca on structure and properties and to make reference to the investigations carried out by F. Romankiewicz [16].

The mechanical properties obtained (Table 4) are in respect of R_m, A and Z much higher than those imposed by the forner Polish Standard PN-H-87026:1979 (for castings made in sand moulds the minimum values should be: R_m= 500 MPa, $R_{0,2}$ = 180 MPa, A_5 = 15% and HB = 110); the situation is similar in the case of the corresponding Japanese CuAl8-10Fe1-4Mn0.1-1.0 alloy (R_m= 490 MPa, A = 20% and HB = 90 according to the Standard JIS H-5114). In some cases the obtained values of $R_{0,2}$ were slightly lower than the required ones. The differences between the individual melts are very small which indicates similar effect of the alternatively used additives of Na, K, or Ca.

Table 4. Mechanical as-cast properties of CuAl10Fe3Mn2 bronze modified with sodium (M), potassium (N) and calcium (P); mean results from 3 measurements

Tabela 4. Właściwości mechaniczne w stanie po odlaniu brązu CuAl10Fe3Mn2 modyfikowanego sodem (M), potasem (N) i wapniem (P); wyniki średnie z trzech pomiarów

Sample designation	$R_{0,2}$ MPa	R_m MPa	A_5 %	Z %	Maximum values $R_{0,2}/R_m/A_5/Z$	Hardness HB 2.5/187.5		
						Mean from 3 measurements	$HB_{śr}$ [1]	Scatter HB [2] min/max
Ma [3]	176.7	605	25.0	26.9	182.2/611/26.4/29.4	168.3-178.6	172.2	163-180
Mb	180.0	607	27.0	26.0	180.9/611/27.0/26.0	169.3-174.3	172.3	166-188
Mc	177.9	596	27.5	27.1	179.6/611/34.0/29.4	158-172.6	164.9	153-174
Na	176.0	595	24.9	23.2	183.4/599/29.0/29.4	167.6-172.0	170.2	157-179
Nb	175.4	611	26.9	26.6	177.1/611/27.4/27.8	165.3-172.6	170.0	158-175
Nc	179.6	607	28.3	26.6	179.6/611/34.0/31.0	166.0-172.0	169.7	163-179
Pa	178.3	599	22.8	22.5	178.3/611/23.8/24.3	166.6-177.6	171.8	161-179
Pb	180.5	575	21.2	23.7	180.9/580/211/24.3	160.6-171.0	166.3	158-172
Pc	181.5	583	24.1	25.2	183.5/586/26.0/26.1	163.0-166.3	164.7	158-170

[1] mean from mean values, i.e from 9 measurements
[2] values from individual measurements
[3] a,b,c denote the successive samples from a given melt (M-N or P)

The effectiveness of modification process can be evaluated from the residual content of modifier, and this amounted to 0.0013% Na, 0.0003% K, or 0.031–0.034% Ca, respectively.

4. Conclusions

A. The conclusions from stage I of the research, based on the examinations of microstructure, suggested the selection for further investigations of additives belonging to the modifiers of type I.
The reasons of this choice were the following:

- visible spheroidising of phase α,
- more uniform distribution of iron-rich phases,
- considerable reduction of oxide inclusions, combined with simultaneous deoxidising effect of elements, specially of Ca,
- the lack in practical application and in studies done so far of modifiers for aluminium bronzes.

B. The thermal analysis can provide valuable information, specially on the eutectoid transformation, the length of eutectic arrest, and the solidification and cooling rate (from the end of eutectic arrest). Because pouring temperatures differed - though very little only - the length of the section on the solidification and cooling curve pertinent to the eutectic is not fully useful in the evaluation; the cooling rate v'_{sr}, on the other hand, is important in this evaluation, and the higher are its values, the greater is the tendency to a higher rate of crystallisation with all the consequences that it has for the grain size.

The eutectic arrests approach the equilibrium temperature (1037°C) and amount to: B - 1035°C, C - 1037°C, D - 1038°C, E - 1038°C, F - 1039°C, G - 1038°C and H -1039°C, and so their variability ranges from 1035 to 1039°C. With exception of the Na addition, all other additives are characterised by the temperature of eutectic transformation only slightly higher than the equilibrium point.

On the other hand, in the case of casting into sand moulds and sand moulds with insulating material, the deviations from the equilibrium eutectic arrest are much greater in respect of both temperature and frequent deviations from the horizontal run, specially in the case of moulds with insulating layer.

In evaluating the length of eutectic arrest very suitable is also the analysis of the run of function $dT/dt = f(t)$.

C. To obtain greater variations in heat transfer rate, the test castings were poured in dies, in sand moulds, and in sand moulds with insulating material. The differences in structure are quite obvious as well as the differences between the centre and edge of specimens.

D. To trace the solid state changes of structure, dilatometric and calorimetric examinations were carried out. In particular, the analysis of $\beta(T\text{-}T_o) = f(T)$ curve and of the calorimetric curve enabled a very sensitive evaluation of the solid state transformations.

E. An analysis of the run of the curves of temperature gradients confirms that the differences in heat transfer rate are quite significant in the case of die and sand mould castings (up to 10 times), and relatively small when castings are made in sand moulds and in sand moulds with insulating material. Very interesting is the configuration of gradient curves - it is similar for die castings, while revealing some deviations for sand moulds.

F. The mechanical properties obtained at stage II of the research show only slight diffe-

rences in castings with different levels of the Na, K and Ca additives. All reveal the mechanical properties (R_m and hardness HB) higher than the values predicted by respective standards; the plastic properties (A_5, Z) are even much higher. Proof stress ($R_{0,2}$), on the contrary, is slightly lower than the value required by the standard. So, these are the relatively high mechanical properties, while plastic properties make the material suitable for applications under dynamic loads.

G. At both stages I and II of the research, a high melting loss of Na, K and Ca was observed, which accounts for the fact that the residual content of these elements in melts, and consequently in castings, is low.

H. Basing on the results of the conducted research, a beneficial effect of the type I modifiers addition has been stated.

I. The applied double deoxidising of melts B-H is important for protection against oxidation during melting and refining. In practice, the preparation of well deoxidised molten metal consists in deoxidising the melt after melting and overheating, followed by deoxidising it once again after refining with nitrogen. Very encouraging results were obtained using different deoxidiser, e.g. phosphorus first, and magnesium next.

Acknowledgements

The results of the studies related in this article have been taken from a report of the Research Project No. 4T08A 026 25, sponsored by the Ministry of Science and Higher Education, entitled: “Stimulating the mechanism of $\alpha+\beta$ eutectic formation in Cu-Al system through control of thermal parameters and grain refining in α phase combined with modification of $\alpha+\beta$ ($\alpha+\gamma_2$) eutectic structure in experimental research and computer simulation”.

References

1. Cibula A.: J. Inst. Met. Vol. 82. VII 1954, 513-524; FTJ 1955, Vol. 30, 713–726
2. Reynolds & Tottle A.: J. Inst. Met. 1951, Vol. 80, 93–98
3. French A.R., Cibula A.: Metalurgia IX 1968, 91–93
4. Stolarczyk E.: Brit.Foundr. IX 1961, 377–382
5. Mannheim R., et al. Giessereiforschung; Vol. 40, 1/1988, 1–16
6. Romankiewicz F., Głazowska I., Rybakowski M.: Metall, 48, 1/1994, 865–871
7. Sadayappan M., Faoyinu F.A., Sahoo M.: Int. Workshop on Permanent Mold Casting of Copper – Base Alloys, Ottawa 15-16 October 1993, 45–48
8. Sadayappan M., Cousineau D., Zavodil R., Sahoo M., Michels H.: AFS Trans., No.108, 2002, 505–514
9. Heike R.: Bul. De Documentation Technique, No. 33, II 1960, 13–15
10. Sadayappan M., Fasoyinu F.A., Thompson J., Sahoo M.: AFS Trans. Vol., 107, 1999, 337–342
11. Reif W., Weber G.: Metall, No. 41, Vol. 11, XI 1987, 1131–1137
12. Romankiewicz F., Ellerbrok R., Engler S.: Giesserei-Forschung, Vol. 89, 1/1987, 25–33
13. Couture A., Edwards J.O.: AFS Trans, No. 114, 1973, 453–461

14. Stucky M.: Bul. De Documentation Technique CTIF, 2004, 45–53
15. Romankiewicz F.: Rudy i Metale Nieżelazne 20, 2/1979, 25 and 5/1980, 193–196
16. Bydałek A.: Rudy i Metale Nieżelazne 23, 5/1978, 222–227
17. Romankiewicz F.: Prz. Odl. 27, 10/1978, 239–242 and 30, 4/1981, 128–131
18. Górny Z., Kluska-Nawarecka S., Połcik H.: Archiwum Odlewnictwa, Vol. C, No. 18, 2006, 239-238 (paper presented at the Podbańska Conference)
19. Gazda A., Górny Z., Kluska-Nawarecka S., Miętka Z., Wacławik Z., Warmuzek M.: Prace Inst.Odlewnictwa, 1-2/1998, 31–53
20. Stucky M.: Fonderie, Fondeur d'Aujourd` hui, no. 218 (2002), 34–40
21. Sahoo M., Couture A.: Giesserei-Praxis, 1–2/1985, 8–17
22. Dubois B., Ocampo B.: Fonderie. Fondeur d`Aujourd`hui, 12/1982, 33–39
23. Hansen M., Anderko K.: Constitution of Binary Alloys, McGraw-Hill Book Comp. New York 1958 and G.V.Raynor: Inst. of Metals 1946
24. AFS-Handbook Vol. III, 1992
25. Gazda A., Górny Z., Kluska-Nawarecka S., Połcik H., Romankiewicz F., et al.: Research Project KBN 4 TO8A 026 25, 2003–2006
26. Edwards J.O., Whittaker D.A.: AFS Trans., 69 (1961), 862–872
27. Białas K., Ziemba H.: Rudy i Metale Nieżelazne, 24, 10/1989, 367–371
28. Sędzimir A., Madej W.: A study of Foundry Research Institute no. 0/5871, Kraków 1995 entitled: „Badania brązów specjalnych jako tworzywa na kokile"
29. Benkisser G., Winhel G.: Metall 49, 4/1995, 288–273
30. Sadayappan M., Zavadil R., Sahoo M.: AFS Trans., (2001), 745–758
31. Thomson R., Edwards J.O.: AFS Trans., 86 (1978), 385–394
32. Sahoo M.: Giesserei-Praxis, 23-24/1983, 365–376
33. Benkisser G., Winkel G., Hovn-Samodelkin G.: Metall 49, 4/1995, 268–273
34. Wolf K.P., Wagner D., Wilhelm S.: Giessereitechnik 36, 6/1990, 178–181
35. Horn-Samodelkin G., Winkel G., Rühl I.: Metall, 50, 1/1996, 44
36. Kowarsch A.: Prz.Odl., 4/1984, 128–135
37. Gałuszko M., Haimann K., Kordasz S., Pękalski G.: Ochr. Koroz. 33, 3/1990, 55–60
38. Czapliński J., Pękalska I., Pękalski G.: Rudy i Metale Nieżelazne 29, 3/1984, 105-110 and 31, 5/1986, 147–152
39. Górny Z., Sobczak J.: Nowoczesne tworzywo odlewnicze na bazie metali nieżelaznych, Za-pis Kraków, 2005
40. Górny Z.: Odlewnicze brązy aluminiowe (monograph), Instytut Odlewnictwa, Kraków, 2006

Reviewer: prof. dr hab. inż. Andrzej Białobrzeski